# Blood flow rate and wall shear stress in seven major cephalic arteries of humans

**Roger S. Seymour[1*], Qiaohui Hu[1] and Edward P. Snelling[2,3]**

[1]University of Adelaide, School of Biological Sciences, Faculty of Sciences, Adelaide, 5005, South Australia, Australia

[2]University of Pretoria, Department of Anatomy and Physiology, Faculty of Veterinary Science, Onderstepoort, 0110, South Africa

[3]University of the Witwatersrand, Brain Function Research Group, School of Physiology, Faculty of Health Sciences, Johannesburg, 2193, South Africa.

*Corresponding author: roger.seymour@adelaide.edu.au

**Abstract**

Blood flow rate ($\dot{Q}$) in relation to arterial lumen radius ($r_i$) is commonly modelled according to theoretical equations and paradigms, including Murray's Law ($\dot{Q} \propto r_i^3$) and da Vinci's Rule ($\dot{Q} \propto r_i^2$). Wall shear stress ($\tau$) is independent of $r_i$ with Murray's Law ($\tau \propto r_i^0$) and decreases with da Vinci's Rule ($\tau \propto r_i^{-1}$). These paradigms are tested empirically with a meta-analysis of the relationships between $\dot{Q}$ and $r_i$ in seven major arteries of the human cephalic circulation from 19 imaging studies in which both variables were presented. The analysis shows that $\dot{Q} \propto r_i^{2.16}$ and $\tau \propto r_i^{-1.02}$, more consistent with da Vinci's Rule than Murray's Law. This meta-analysis provides standard values for $\dot{Q}$, $r_i$ and $\tau$ in the human cephalic arteries that may be a useful baseline in future investigations. On average, the paired internal carotid arteries (ICAs) supply 75%, and the vertebral arteries (VAs) supply 25%, of total brain blood flow. The ICAs contribute blood entirely to the anterior and middle cerebral arteries and also partly to the posterior cerebral arteries via the posterior communicating arteries of the Circle of Willis. On average, the ICAs provide 88% of the blood flow to the cerebrum and the VAs only 12%.

**Key words:** artery; brain; cardiovascular; cerebral; da Vinci's Rule; Murray's Law

**Running title:** Blood flow and shear stress in cephalic arteries

## Introduction

The structure of the arterial tree has attracted the attention of scholars for centuries. Even before the blood was shown to circulate by Harvey in 1628 (Willis, 2016), Leonardo da Vinci described the branching of the arteries in mathematical terms, indicating that the cross-sectional area of a parent artery was equal to the sum of the cross-sectional areas of the two daughter arteries branching from it (Richter, 1970), a relationship that is now called "da Vinci's Rule". In other words, the square of the diameter of a parent artery should be equal to the sum of the squares of the diameters of the two daughter arteries. More than three centuries later, in an attempt to analyse the structure of the arterial tree as an efficient energy-conserving system, Cecil Murray proposed that, to minimise energy losses, the cube of the diameter of the parent artery should be equal to the sum of the cubes of the diameters of the two daughter arteries, a relationship that became known as "Murray's Law" (Murray, 1926). Murray's Law was a formal treatment of what was proposed by Thomas Young in 1808, that is, the ratio of the diameters of the parent and daughter vessels is $2^{1/3}$ : 1 (Sherman, 1981). Mathematically, these paradigms can be expressed in terms of vessel radius, and represent two cases of the general relationship:

$$r_p^n = r_{d1}^n + r_{d2}^n \quad (1)$$

where $r_p$ is the radius of a parent artery, $r_{d1}$ and $r_{d2}$ are the radii of its two daughter arteries, and *n* is 2 for da Vinci's Rule and 3 for Murray's Law.

It is clear that characteristic arterial size is determined by dynamic remodelling of the vessel diameter in response to blood velocity near the wall (Langille, 1996, Simons et al., 2016). The force of blood flowing over the endothelial surface interacts with a junctional mechanosensory complex involving VEGFR protein that effects adjustments of wall dimensions to normalise the velocity near the wall (Baeyens et al., 2015). The normal "set-point" is considered a regulated value of wall shear stress (WSS; dyn $cm^{-2}$). WSS can be evaluated from haemodynamic theory (Secomb, 2016). The famous haemodynamic paradigm that relates laminar flow rate to vessel size is the Poiseuille-Hagen (P-H) equation, which is a solution to one of the incompressible Navier-Stokes equations:

$$\Delta P = (8 \dot{Q} \eta L)/(\pi r_i^4) \quad (2)$$

where $\Delta P$ is the pressure difference required to achieve a rate of laminar flow ($\dot{Q}$) of a fluid of given viscosity ($\eta$) in a straight, horizontal tube of length (L) and inner radius ($r_i$). The pressure (P = force/area) driving flow acts on the cross-sectional area of the tube ($A = \pi r_i^2$), yielding a force ($F_p$):

$$F_p = A \Delta P = (\pi r_i^2) (8 \dot{Q} \eta L)/(\pi r_i^4) = (8 \dot{Q} \eta L)/r_i^2 \quad (3)$$

The flow creates a balancing frictional force ($F_\tau$) which equals WSS ($\tau$) occurring along the total inner surface area of the tube ($S = 2 \pi r_i L$):

$$F_\tau = S \tau = 2 \pi r_i L \tau \quad (4)$$

Because $F_p = F_\tau$, so

$$\tau = ((8 \dot{Q} \eta L)/r_i^2)/(2 \pi r_i L) = (4 \dot{Q} \eta)/(\pi r_i^3) \quad (5)$$

Equation (5) is attributed to Poiseuille, but for distinction from the P-H equation, we have previously called it the "shear stress equation" (Seymour et al., 2015, Seymour et al., 2016). In imaging studies, WSS can also be calculated from the derivative of the velocity gradient near the wall, and the results largely concur with values calculated from the shear stress equation in the common carotid artery (Zarins et al., 1983). For physiological studies, eq. (5) is more useful than the simplified version, $\tau = (r_i \Delta P)/(2 L)$, because $\Delta P$ and L are difficult to evaluate.

If, for any artery, $\dot{Q} \propto r_i^n$, then $\tau \propto r_i^{n-3}$. In particular, if *n* = 3, as in the case of Murray's Law, then $\dot{Q} \propto r_i^3$ and $\tau \propto r_i^0$; the exponent of 0 indicates that WSS is a constant throughout the arterial tree. Under da Vinci's Rule, *n* = 2 and so $\dot{Q} \propto r_i^2$ and $\tau \propto r_i^{-1}$; the negative exponent indicates that WSS decreases in larger vessels of the arterial tree.

The literature has conflicting information on the scaling of arterial size and blood flow rates. Much of the 20th century literature assumed that arterial WSS is constant at about 10-20 dyn $cm^{-2}$, implicitly affirming Murray's Law (Ku, 1997). However, natural selection does not necessarily

conform to single factors, nor is it necessary for the value of the exponent *n* to be a constant throughout the arterial tree. In fact, *n* generally varies between 2 and 3 in experimental studies, but it is uncertain how *n* varies predictably in real arteries (Karau et al., 2001).

Murray's Law is upheld in studies of the small-medium arteries where the exponents *n* are nearly 3 for blood flow rate in relation to arterial diameter, and nearly zero for WSS. For example, flow rate varies with diameter to the 2.76 power in human retinal arteries (Riva et al., 1985), similar to retinal arteries of rhesus monkeys (Zamir and Medeiros, 1982). Blood flow in cremaster muscle arteries of rats scales with diameter to the 3.01 power (Mayrovitz and Roy, 1983). Blood flow in pial arteries on the surface of the brain of cats scales with diameter to the 2.98 power (Kobari et al., 1984).

Conversely, da Vinci's Rule has received partial support by several investigators who have shown that WSS is not constant in the major arteries of humans and other mammals. In human studies, WSS varies between 2.9 to 15 dyn $cm^{-2}$ in the aorta and its immediate branches, and WSS decreases in arteries of larger radius according to a power of -0.5 (Cheng et al., 2007). Interspecific studies also indicate that WSS is not a constant in individually named arteries (aortas and carotid arteries) of different-sized mammals, but decreases allometrically with increasing body mass to the approximate power of -0.2 (Greve et al., 2006, Cheng et al., 2007, Weinberg and Ethier, 2007).

Part of the variability in arterial radius, blood flow rate, and WSS undoubtedly relates to the fact that metabolic rates of some tissues are extremely variable, in particular the locomotory muscles. Flow rate in the femoral artery can increase 10-fold between rest and activity (Jorfeldt and Wahren, 1971); the femoral artery therefore shows low WSS at rest, but during activity, values are comparable to those in the similarly-sized common carotid artery (Kornet et al., 2000). In contrast, brain perfusion is well autoregulated, varying less than approximately 20% regardless of whether a person is resting, physically or mentally exercising, or sleeping (Sokoloff et al., 1955, Armstrong, 1983, Hellström et al., 1996, Ogoh and Ainslie, 2009, Sato and Sadamoto, 2010, Hiura et al., 2014). The diameters of the cerebral arteries also change very little between rest and activity (Hellström et al., 1996) or in response to physiological changes in blood pressure and blood gas levels (Payne, 2016). Therefore, a tighter pattern of arterial variables, such as size, flow rate and WSS, may emerge in the circulation to the brain.

Nonetheless, there is disagreement about the scaling pattern in the major arteries of the human cerebral circulation. For example, a study that measured the lumen radii of the parent and branch arteries of the internal carotid, anterior cerebral and middle cerebral arteries from angiographs of healthy individuals found that the branching exponent *n* was $2.9 \pm 0.7$ ($\pm$ SD), thus implying that Murray's Law prevails and WSS is constant (Rossitti and Löfgren, 1993). Another study of blood flow rate and cross-sectional area (A) of the human internal carotid artery and vertebral artery also supported Murray's Law with flow being proportional to $A^{1.84}$, which corresponds to a

very high *n* = 3.74 (Cebral et al., 2008). In contrast, the branching exponent for lumen diameter in these three major cerebral arteries has been measured as 2.06, and the flow rate exponent as 2.45, thereby indicating that WSS increases in the smaller arteries and supporting da Vinci's Rule more than Murray's Law (Chnafa et al., 2017).

The present investigation is a meta-analysis of 19 imaging studies of blood flow rate and size in seven major cephalic arteries of humans. It analyses the relationships between all of the major arteries supplying the brain, and it represents the largest sample of studies that provide data for both flow rates and artery sizes in the same publication. It was gathered to test the applicability of Murray's Law and da Vinci's Rule in a system of relatively constant blood flow and to establish an empirical dataset useful for estimation of blood flow rate from measurements of cephalic arterial size in humans.

## Methods

The literature was searched for studies involving *in vivo* measurements of major cephalic arteries from humans, including the common carotid (CCA), internal carotid (ICA), vertebral (VA), basilar (BA), anterior cerebral (ACA), middle cerebral (MCA) and posterior cerebral arteries (PCA). Techniques included phase-contrast magnetic resonance imaging (PC-MRI), transcranial Doppler ultrasound (TCD), multi-gate spectral Doppler ultrasound (MSDU), color duplex Doppler ultrasound (CDDU) and high resolution ultrasound (HRU). Very many papers were screened, but studies were accepted only if they reported paired values for *both* blood flow rate and arterial lumen size under normal arterial blood pressure, so that WSS could be calculated independently for individual publications. There was no *a priori* reason to dismiss certain studies, so all data meeting these criteria were accepted as reported. Some variation may have resulted from differences in technique or image resolution, but there is no significant difference if exclusively PC-MRI studies are used in the analysis compared to ultrasound studies (see results). No weighting of studies with different sample sizes was undertaken to avoid pseudo-replication involving techniques, laboratories, subject populations, etc. The object of the meta-study was to treat an individual study as a single datum for each reported artery.

Blood flow rates were taken as reported means from presumably healthy adult individuals (control or disease-free groups). In a few cases, flow rate was calculated from mean velocity multiplied by cross-sectional lumen area. Arterial lumen radius was calculated from either diameter or cross-sectional area of *in vivo* images. WSS was calculated from each pair of data using the shear stress equation (eq. 5), assuming a constant blood viscosity of 0.04 dyn s $cm^{-2}$ (Schmid-Schönbein et al., 1969, Amin and Sirs, 1985). This equation ignores actual viscosity at the wall, which may be slightly lower than the blood in general, as well as velocity changes during the cardiac cycle, blunted velocity profiles that occur in major arteries, and effects due to curves and bifurcations (Reneman et

al., 2009). However, flow in the measured arteries is essentially laminar (Winkel et al., 2015) and effectively Newtonian (McGah and Capobianchi, 2015). If a full parabolic profile is assumed, according to Poiseuille flow conditions, the WSS may be underestimated (Dammers et al., 2003, Reneman et al., 2009). Measured *in vivo* velocity profiles for the human carotid artery that account for these factors yield WSS values of 11 – 13 dyn $cm^{-2}$ (Reneman and Hoeks, 2008, Reneman et al., 2009). We found that the mean from seven common carotid artery WSS values in the present study was within this range (12.01 dyn $cm^{-2}$), providing confidence that our method is accurate and valid to calculate the scaling exponent of WSS on arterial radius.

Values are presented as means with 95% confidence intervals (CI), and are compared with ANOVA calculated with Microsoft Excel add-in StatistiXL (www.statistixl.com). Arithmetic data were plotted on arithmetic axes and power equations fitted with graphing and statistical software (GraphPad Software Inc., La Jolla, CA, USA).

## Results

Paired data for blood flow rate ($\dot{Q}$, $cm^3\ s^{-1}$) and arterial lumen radius ($r_i$, cm) were obtained from 19 imaging studies involving major arteries of the human cephalic circulation of healthy adult individuals (raw data available in Supplementary Material). The means and 95% CIs of $\dot{Q}$, $r_i$ and calculated WSS ($\tau$, dyn $cm^{-2}$) are given in Table 1. (Data for exclusively PC-MRI studies are presented in Supplementary Material Table S2, but they are not significantly different from the entire set. For example, $\dot{Q}$ in the ICA averaged 3.95±0.55 $cm^3\ s^{-1}$ in seven studies involving PC-MRI and 4.18±0.35 $cm^3\ s^{-1}$ in six studies that used ultrasound (t-test: P = 0.52). Other arteries were represented in fewer studies, also with no significant differences.)

The contributions of each cephalic artery to total brain blood flow are summarised in Table 2. The two ICAs supply 75%, and the two VAs supply 25%, of total brain blood flow. Single ICA flow (4.05 $cm^3\ s^{-1}$) is slightly greater than the sum of single ACA+MCA flows (3.62 $cm^3\ s^{-1}$), and slightly less than the sum of single ACA+MCA+PCA flows (4.61 $cm^3\ s^{-1}$). However, the lower 95% confidence limit of individual ICA flow is 3.72 $cm^3\ s^{-1}$, which is greater than ACA+MCA flows, but less than ACA+MCA+PCA flows (Table 1). This indicates that, on average, the ICA contributes blood entirely to the ACA and MCA, and also partly to the PCA through the posterior communicating artery (PCoA) of the Circle of Willis (Fig. 1). The VA also contributes to the PCA, as well as to the arteries of the upper spinal cord, brainstem and cerebellum. Thus the ICAs account for 88%, and the VAs account for 12%, of cerebral perfusion.

The mean ICA flow (4.05 $cm^3\ s^{-1}$) is about one-half of that of the CCA (8.09 $cm^3\ s^{-1}$), and the difference (4.04 $cm^3\ s^{-1}$) should equal flow to the external carotid artery (ECA), which is nearly equal to ICA flow. However, published measurements of ECA flow rate are about 51 - 65% of that in the ICA on the same side (Schöning et al., 1994, Scheel et al., 2000, Hoi et al., 2010). The discrepancy is

possibly attributed to branching of the superior thyroid artery, the lingual artery and the ascending pharyngeal artery from the ECA, which occurs close to its junction with the ICA (Fig. 1). It is possible that published measurements of ECA flow were made above this branching.

Calculated WSS is lowest in the larger CCA and VA, and highest in the smaller MCA and ACA (Table 1). A full-factorial ANOVA and Student-Newman-Keuls *post hoc* test show that WSS is significantly higher ($P < 0.05$) in the MCA and ACA than in the other arteries (except for the MCA and BA that are close to significant; $P = 0.07$). WSS in the MCA and ACA are not significantly different from each other ($P = 0.92$). WSS in the PCA is not significantly different from that in other arteries, however the sample size for this artery is low (N = 3 studies).

Mean values of flow rate ($\dot{Q}$, $cm^3\ s^{-1}$) and WSS ($\tau$ , $dyn\ cm^{-2}$) are plotted in relation to lumen radius ($r_i$, cm) in Figure 2. Allometric power equations, derived from 7 data points, for the cephalic arteries of humans are: $\dot{Q} = 82.6\ r_i^{2.16 \pm 1.13\ (95\%\ CI)}$ ($R^2 = 0.83$) and $\tau = 3.44\ r_i^{-1.02 \pm 1.29}$ ($R^2 = 0.45$). Alternatively, polynomial regression equations ($\log \dot{Q} = -0.20 \log r_i^2 + 1.91 \log r_i + 1.82$, and $\log \tau = -0.20 \log r_i^2 - 1.09 \log r_i + 0.53$), derived from a larger analysis of 20 named arteries in nine species of mammals (Seymour *et al*. 2019), describe the human data well. Indeed, the sums of squared residuals of the logged flow rate data are nearly identical for the two models (0.115 for the interspecific polynomial regression equation and 0.107 for the human power equation). Focusing on patterns within individual arteries, there is no obvious relationship between $\dot{Q}$ and $r_i$ (Fig. S1A), but a clear, inverse relationship appears between WSS and $r_i$ (Fig. S1B).

## Discussion

### Patterns of cranial blood flow

The primary motivation for this meta-analysis was to establish standard values for blood flow rate and arterial size in the major cephalic arteries of humans. This analysis includes 19 imaging studies of seven main arteries, compared to a previous meta-analysis of six studies of the common carotid artery only (Cheng et al. 2007). Only one of the 19 studies included all seven arteries (Zhao et al 2015). Thus the present analysis goes as far as possible to reduce potential bias in individual studies and produce the best summary so far. The results are useful as a baseline against which future investigations can be compared, for example, clinical human studies and those concerning human evolution.

The literature indicates that there is little net flow of blood from one side of the brain to the other when the Circle of Willis is complete. Previous studies show that flow rates are nearly identical in the left and right ICAs, but not necessarily in the VAs (Enzmann et al., 1994, Schöning et al., 1994, Sato and Sadamoto, 2010, van Ooij et al., 2013, Zhao et al., 2015). This aligns well with measurements of the nearly-equal sizes of unpressurised cerebral arteries in the two hemispheres

(Burlakoti et al., 2017, Burlakoti et al., 2018). Importantly, the ICA supplies the ACA and the MCA that service most of the cerebral cortex. The PCA receives blood mainly from the VA and supplemented by the ICA via the PCoA, and calculations based on our mean values indicate that the cerebrum receives 88% of its perfusion from the ICAs and only 12% from the VAs. This provides confidence that estimates of blood flow rates derived from ICA foramen size captures the majority of cerebral perfusion and well represents cerebral metabolic rate in hominins among the primates (Seymour et al., 2015, Seymour et al., 2016).

The low contribution by the VAs in humans is associated with variability in flow patterns among individuals. Flow rates in the PCoAs that connect the ICAs to the PCAs are small and apparently not essential. Flow along the PCoAs can be in either direction and is unpredictable in individuals that have either one or two of these arteries (Klötzsch et al., 1996, van Ooij et al., 2013). One or both of the PCoAs are absent in about 25% of humans (Lippert and Pabst, 1985). In contrast, absence of the ICAs is very rare, loss of one ICA occurring in less than 0.01%, and two ICAs in less than 0.001%, of the population (Alexandre et al., 2016).

**da Vinci's Rule and Murray's Law**

The paradigms describing the circulation assume that it is a series of fractally bifurcating tubes. Although the major cephalic arteries do not conform to this model, but are rather a non-fractal, anastomosing network in which the arteries communicate in the Circle of Willis (Fig. 1), we assessed it as if they conformed, being partly justified by the fact that there is little net flow between hemispheres and cephalic flow rates are remarkably constant. Therefore, the working hypotheses are that the data for artery sizes and flow rates should have exponents of $n = 2$ for da Vinci's Rule or $n = 3$ for Murray's Law.

The exponent for blood flow rate in relation to lumen radius derived from the human cephalic arteries is 2.16 ± 1.13 (Fig. 2A), and the exponent for calculated WSS is -1.02 ± 1.29 (Fig. 2B). Although the 95% CI values include 3.0 or 0.0, respectively, the exponents are in much closer agreement to da Vinci's Rule than Murray's Law. Increasing WSS in smaller cephalic arteries is similar to the results of a previous study of the ICA, MCA and ACA only (Chnafa et al., 2017). The two studies are also similar in showing a steep inverse relationship between WSS and radius between artery groups (Fig. S1B). We suspect that this is an artefact related to study-specific differences in measurement of lumen radius. Radii of all of these arteries are always highest in two studies (Zhao et al., 2015, Enzmann et al., 1994) and always lowest in three studies (Bouillot et al., 2018, Chnafa et al., 2017, Fahrig et al., 1999), yet the flow rates are similar. This underscores the value of this meta-study. There are investigations of size and flow in human cephalic arteries that show similar increases in WSS in smaller vessels, but do not comment specifically on da Vinci's Rule or Murray's Law (Enzmann et al., 1994, Fahrig et al., 1999, Reymond et al., 2012, van Ooij et al., 2013, Zhao et al., 2015). All of these studies are contrary to the conclusions of constant WSS in these vessels (Rossitti and Löfgren, 1993) and the cubic scaling of flow and diameter of the VA and ICA (Cebral et al., 2008).

The power equations set to the data in this analysis conform well to recent mathematical theory and to empirical results from mammals in general. In particular, the exponent of 2.16 for flow rate on radius (Fig. 2A) is similar to the exponent of 2.33 expected by recent haemodynamic theory of fractal-branching arterial trees (Huo and Kassab, 2012, Huo and Kassab, 2016). The present data are a subset of a larger study of arterial flow rate and WSS on lumen radius derived from 20 named systemic arteries among nine species of mammals (Seymour *et al.* 2019). That study confirms that a single exponent should not be applied to a broad range of arterial size and that a second-order polynomial equation best describes the log-transformed interspecific data. The derivative of the interspecific equation (the slope of the curve at any point) is equivalent to the exponent of a power equation at that point. The derivative is approximately 2.1 for the largest artery in this study (CCA $r_i$ = 0.327 cm) and 2.3 for the smallest (PCA $r_i$ = 0.150), so 2.16 is a reasonable exponent for these arteries. By comparison, the derivative is near 3.0 in very small arteries such as in the cremaster muscle of a rat, decreasing to about 2.0 in the aorta of a human (Seymour et al. 2019). Thus da Vinci's Rule may be applied to large arteries and Murray's Law to small ones.

The failure of the major arteries of the cephalic circulation to conform to Murray's Law does not entirely invalidate the idea that the structure of the circulatory system results in the least energy required by the heart. Our results are related to different functions of major and peripheral arteries. The major arteries, including those assessed in the present meta-analysis, buffer pulsatile pressures from the heart and minimise energy loss to reflected waves (Savage et al., 2008, Newberry et al., 2015), whereas the peripheral arteries distribute the blood according to the demands of the tissues and reduce the velocity to allow time for gas exchange (Zamir, 2001). It is clear that Murray's Law applies well in the peripheral arteries that are the major source of resistance to flow (Womersley, 1955, Sherman, 1981, Zamir et al., 1992, Savage et al., 2008, Reneman et al., 2009, McGah and Capobianchi, 2015). Low resistance in the major arteries is indicated by a small drop in mean blood pressure of approximately 5 mmHg between the aortic root and the MCA (Reymond et al., 2012). Murray considered two factors to be important in affecting the structure of the circulatory system – energy costs associated with pumping blood and energy costs of building and maintaining the blood and vessels (Zamir, 1977). It is not clear which factor has more influence, with some modelling favouring pumping costs (Price et al., 2007) and others favouring material costs (Tekin et al., 2016). It is possible that the most important factor depends on the level of branching.

**Conclusion**

In summary, blood flow to the human brain is relatively constant and occurs through arteries that are usually bilaterally symmetrical. The ICAs supply 88% of the perfusion of the cerebral (cognitive) part of the brain. Among all of the seven major cephalic arteries, the relationship between blood flow rate and arterial size lies closer to da Vinci's Rule than to Murray's Law. Wall shear stress is not constant, but increases in smaller arteries supplying the brain.

**Acknowledgements**

We thank Professor Timothy J. Pedley, Associate Professor Jens Christian Brings Jacobsen and an anonymous referee for advice on the manuscript and Thomas Nelson for help with the literature. This study was supported by the Australian Research Council with a Discovery Grant DP170104952 to R.S.S.). Q.H. holds an Australian Postgraduate Award.

**Author contributions**

R.S.S. developed the original concept, gathered the literature and wrote the first draft. Q.H. and E.P.S. contributed to library research, data analysis, and manuscript writing. All authors gave final approval of the manuscript.

**Electronic Supplementary Material**

The raw data and their literature sources. Individual graphed data (Fig. S1). Results of PC-MRI data only (Table S2).

**Literature cited**

Alexandre AM, Visconti E, Schiarelli C, Frassanito P, Pedicelli A (2016) Bilateral internal carotid artery segmental agenesis: Embryology, common collateral pathways, clinical presentation, and clinical importance of a rare condition. *World Neurosurgery,* **95,** 620.e9-620.e15.

Amin TM, Sirs JA (1985) The blood rheology of man and various animal species. *Quarterly Journal of Experimental Physiology and Cognate Medical Sciences,* **70,** 37-49.

Armstrong E (1983) Relative brain size and metabolism in mammals. *Science,* **220,** 1302-1304.

Baeyens N, Nicoli S, Coon BG, et al. (2015) Vascular remodeling is governed by a VEGFR3-dependent fluid shear stress set point. *Elife,* **4,** e04645

Bouillot P, Delattre BMA, Brina O, et al. (2018) 3D phase contrast MRI: Partial volume correction for robust blood flow quantification in small intracranial vessels. *Magnetic Resonance in Medicine,* **79,** 129-140.

Burlakoti A, Kumaratilake J, Taylor J, Henneberg M (2018) Asymmetries of total arterial supply of cerebral hemispheres do not exist. *Heliyon* **4,** e01086.

Burlakoti A, Kumaratilake J, Taylor J, Massy-Westropp N, Henneberg M (2017) The cerebral basal arterial network: morphometry of inflow and outflow components. *Journal of Anatomy,* **230,** 833-841.

Cebral JR, Castro MA, Putman CM, Alperin N (2008) Flow-area relationship in internal carotid and vertebral arteries. *Physiological Measurement,* **29,** 585-594.

Cheng C, Helderman F, Tempel D, et al. (2007) Large variations in absolute wall shear stress levels within one species and between species. *Atherosclerosis,* **195,** 225-235.

Chnafa C, Bouillot P, Brina O, et al. (2017) Vessel calibre and flow splitting relationships at the internal carotid artery terminal bifurcation. *Physiological Measurement,* **38,** 2044-2057.

Dammers R, Stifft F, Tordoir JHM, Hameleers JMM, Hoeks APG, Kitslaar P (2003) Shear stress depends on vascular territory: comparison between common carotid and brachial artery. *Journal of Applied Physiology,* **94,** 485-489.

Enzmann DR, Ross MR, Marks MP, Pelc NJ (1994) Blood flow in major cerebral arteries measured by phase-contrast cine MR. *American Journal of Neuroradiology,* **15,** 123-129.

Fahrig R, Nikolov H, Fox AJ, Holdsworth DW (1999) A three-dimensional cerebrovascular flow phantom. *Medical Physics,* **26,** 1589-1599.

Greve JM, Les AS, Tang BT, et al. (2006) Allometric scaling of wall shear stress from mice to humans: quantification using cine phase-contrast MRI and computational fluid dynamics. *American Journal of Physiology. Heart and Circulatory Physiology,* **291,** H1700-H1708.

Hellström G, Fischer-Colbrie W, Wahlgren NG, Jogestrand T (1996) Carotid artery blood flow and middle cerebral artery blood flow velocity during physical exercise. *Journal of Applied Physiology,* **81,** 413-418.

Hiura M, Nariai T, Ishii K, et al. (2014) Changes in cerebral blood flow during steady-state cycling exercise: a study using oxygen-15-labeled water with PET. *Journal of Cerebral Blood Flow and Metabolism,* **34,** 389-396.

Hoi Y, Wasserman BA, Xie YYJ, et al. (2010) Characterization of volumetric flow rate waveforms at the carotid bifurcations of older adults. *Physiological Measurement,* **31,** 291-302.

Huo Y, Kassab GS (2012) Intraspecific scaling laws of vascular trees. *Journal of the Royal Society Interface,* **9,** 190-200.

Huo YL, Kassab GS (2016) Scaling laws of coronary circulation in health and disease. *Journal of Biomechanics,* **49,** 2531-2539.

Jorfeldt L, Wahren J (1971) Leg blood flow during exercise in man. *Clinical Science,* **41,** 459-473.

Karau KL, Krenz GS, Dawson CA (2001) Branching exponent heterogeneity and wall shear stress distribution in vascular trees. *American Journal of Physiology-Heart and Circulatory Physiology,* **280,** H1256-H1263.

Klötzsch C, Popescu O, Berlit P (1996) Assessment of the posterior communicating artery by transcranial color-coded duplex sonography. *Stroke* **27,** 486-489.

Kobari M, Gotoh F, Fukuuchi Y, Tanaka K, Suzuki N, Uematsu D (1984) Blood flow velocity in the pial arteries of cats, with particular reference to the vessel diameter. *Journal of Cerebral Blood Flow and Metabolism,* **4,** 110-114.

Kornet L, Hoeks APG, Lambregts J, Reneman RS (2000) Mean wall shear stress in the femoral arterial bifurcation is low and independent of age at rest. *Journal of Vascular Research,* **37,** 112-122.

Ku DN (1997) Blood flow in arteries. *Annual Review of Fluid Mechanics,* **29,** 399-434.

Langille BL (1996) Arterial remodeling: relation to hemodynamics. *Canadian Journal of Physiology and Pharmacology,* **74,** 834-841.

Lippert H, Pabst R (1985) *Arterial variations in Man: Classification and frequency,* J.F. Bergmann, Munich.

Mayrovitz HN, Roy J (1983) Microvascular blood-flow: Evidence indicating a cubic dependence on arteriolar diameter. *American Journal of Physiology. Heart and Circulatory Physiology,* **245,** 1031-1038.

McGah PM, Capobianchi M (2015) A modification of Murray's Law for shear-thinning rheology. *Journal of Biomechanical Engineering,* **137**.

Murray CD (1926) The physiological principle of minimum work. I. The vascular system and the cost of blood volume. *Proceedings of the National Academy of Sciences of the United States of America,* **12,** 207-214.

Newberry MG, Ennis DB, Savage VM (2015) Testing foundations of biological scaling theory using automated measurements of vascular networks. *Plos Computational Biology,* **11,** e1004455.

Ogoh S, Ainslie PN (2009) Cerebral blood flow during exercise: mechanisms of regulation. *Journal of Applied Physiology,* **107,** 1370-1380.

Payne S (2016) *Cerebral Autoregulation: Control of Blood Flow in the Brain,* Springer Nature, Switzerland.

Price CA, Enquist BJ, Savage VM (2007) A general model for allometric covariation in botanical form and function. *Proceedings of the National Academy of Sciences of the United States of America,* **104,** 13204-13209.
Reneman RS, Hoeks APG (2008) Wall shear stress as measured in vivo: consequences for the design of the arterial system. *Medical & Biological Engineering & Computing,* **46,** 499-507.
Reneman RS, Vink H, Hoeks APG (2009) Wall shear stress revisited. *Artery Research,* **3,** 73-78.
Reymond P, Perren F, Lazeyras F, Stergiopulos N (2012) Patient-specific mean pressure drop in the systemic arterial tree, a comparison between 1-D and 3-D models. *Journal of Biomechanics,* **45,** 2499-2505.
Richter JP (1970) *The Notebooks of Leonardo da Vinci,* Dover Publications, New York.
Riva CE, Grunwald JE, Sinclair SH, Petrig BL (1985) Blood velocity and volumetric flow rate in human retinal vessels. *Investigative Ophthalmology and Visual Science,* **26,** 1124-1132.
Rossitti S, Löfgren J (1993) Vascular dimensions of the cerebral arteries follow the principle of minimum work. *Stroke,* **24,** 371-377.
Sato K, Sadamoto T (2010) Different blood flow responses to dynamic exercise between internal carotid and vertebral arteries in women. *Journal of Applied Physiology,* **109,** 864-869.
Savage VM, Deeds EJ, Fontana W (2008) Sizing up allometric scaling theory. *Plos Computational Biology,* **4,** e1000171.
Scheel P, Ruge C, Schöning M (2000) Flow velocity and flow volume measurements in the extracranial carotid and vertebral arteries in healthy adults: reference data and the effects of age. *Ultrasound in Medicine and Biology,* **26,** 1261-1266.
Schmid-Schönbein H, Wells R, Goldstone J (1969) Influence of deformability of human red cells upon blood viscosity. *Circulation Research,* **25,** 131-143.
Schöning M, Walter J, Scheel P (1994) Estimation of cerebral blood flow through color duplex sonography of the carotid and vertebral arteries in healthy adults. *Stroke,* **25,** 17-22.
Secomb TW (2016) Hemodynamics. *Comprehensive Physiology,* **6,** 975-1003.
Seymour RS, Angove SE, Snelling EP, Cassey P (2015) Scaling of cerebral blood perfusion in primates and marsupials. *Journal of Experimental Biology,* **218,** 2631-2640.
Seymour RS, Bosiocic V, Snelling EP (2016) Fossil skulls reveal that blood flow rate to the brain increased faster than brain volume during human evolution. *Royal Society Open Science,* **3,** e160305.
Sherman TF (1981) On connecting large vessels to small. The meaning of Murray's Law. *Journal of General Physiology,* **78,** 431-453.
Simons M, Gordon E, Claesson-Welsh L (2016) Mechanisms and regulation of endothelial VEGF receptor signalling. *Nature Reviews Molecular Cell Biology,* **17,** 611-625.
Sokoloff L, Mangold R, Wechsler RL, Kennedy C, Kety SS (1955) Effect of mental arithmetic on cerebral circulation and metabolism. *Journal of Clinical Investigation,* **34,** 1101-1108.
Tekin E, Hunt D, Newberry MG, Savage VM (2016) Do vascular networks branch optimally or randomly across spatial scales? *Plos Computational Biology,* **12,** e1005223.
van Ooij P, Zwanenburg JJM, Visser F, et al. (2013) Quantification and visualization of flow in the Circle of Willis: Time-resolved three-dimensional phase contrast MRI at 7 T compared with 3 T. *Magnetic Resonance in Medicine,* **69,** 868-876.
Weinberg PD, Ethier CR (2007) Twenty-fold difference in hemodynamic wall shear stress between murine and human aortas. *Journal of Biomechanics,* **40,** 1594-1598.
Willis R (2016) *On the Motion of the Heart and Blood in Animals,* Resource Publications, Eugene, Oregon, USA.
Winkel LC, Hoogendoorn A, Xing RY, Wentzel JJ, Van der Heiden K (2015) Animal models of surgically manipulated flow velocities to study shear stress-induced atherosclerosis. *Atherosclerosis,* **241,** 100-110.
Womersley JR (1955) Method for the calculation of velocity, rate of flow and viscous drag in arteries when the pressure gradient is known. *Journal of Physiology-London,* **127,** 553-563.

Zamir M (1977) Shear forces and blood vessel radii in the cardiovascular system. *Journal of General Physiology,* **69,** 449-461.

Zamir M (2001) Fractal dimensions and multifractility in vascular branching. *Journal of Theoretical Biology,* **212,** 183-190.

Zamir M, Medeiros JA (1982) Arterial branching in man and monkey. *Journal of General Physiology,* **79,** 353-360.

Zamir M, Sinclair P, Wonnacott TH (1992) Relation between diameter and flow in major branches of the arch of the aorta. *Journal of Biomechanics,* **25,** 1303-1310.

Zarins CK, Giddens DP, Bharadvaj BK, Sottiurai VS, Mabon RF, Glagov S (1983) Carotid bifurcation atherosclerosis. Quantitative correlation of plaque localization with flow velocity profiles and wall shear stress. *Circulation Research,* **53,** 502-514.

Zhao XX, Zhao MD, Amin-Hanjani S, Du XJ, Ruland S, Charbel FT (2015) Wall shear stress in major cerebral arteries as a function of age and gender--a study of 301 healthy volunteers. *Journal of Neuroimaging,* **25,** 403-407.

Table 1. Mean ± 95% CI arterial lumen radii, blood flow rates, and calculated wall shear stress (WSS) of single arteries of the human cephalic circulation based on data from 19 PC-MRI and ultrasound imaging studies. Data for exclusively PC-MRI studies are given in Table S1 of the Supplementary Material.

| Artery | Number of studies | Radius ($r_i$, cm) | | Flow rate ($\dot{Q}$, $cm^3\ s^{-1}$) | | WSS ($\tau$, dyn $cm^{-2}$) | |
|---|---|---|---|---|---|---|---|
| SINGLE | N | mean | 95% CI | mean | 95% CI | mean | 95% CI |
| common carotid (CCA) | 7 | 0.327 | 0.016 | 8.05 | 1.00 | 12.0 | 2.2 |
| internal carotid (ICA) | 13 | 0.239 | 0.015 | 4.05 | 0.33 | 16.1 | 3.0 |
| basilar (BA) | 3 | 0.190 | 0.021 | 2.39 | 0.29 | 18.2 | 4.1 |
| vertebral (VA) | 8 | 0.186 | 0.014 | 1.37 | 0.21 | 11.3 | 3.0 |
| middle cerebral (MCA) | 7 | 0.159 | 0.021 | 2.41 | 0.42 | 36.2 | 15.7 |
| posterior cerebral (PCA) | 3 | 0.150 | 0.019 | 0.99 | 0.14 | 16.2 | 7.0 |
| anterior cerebral (ACA) | 5 | 0.129 | 0.027 | 1.21 | 0.10 | 35.5 | 18.5 |

Table 2. Mean total blood flow rates of the paired cephalic arteries of humans (= twice the single flow rates). Also shown are the percentage flow rates relative to total brain blood flow rate.

| Variable | $cm^3\ s^{-1}$ | $cm^3\ min^{-1}$ | % total |
|---|---|---|---|
| Total brain flow rate | 10.8 | 650 | 100 |
| ICA × 2 | 8.1 | 486 | 75 |
| VA × 2 | 2.7 | 164 | 25 |
| (ACA+MCA) × 2 | 7.2 | 434 | 67 |
| (ACA+MCA+PCA) × 2 | 9.2 | 553 | 85 |
| PCoA × 2* | 0.9 | 53 | 8 |

*Posterior communicating artery (PCoA) flow is calculated (ICA – ACA – MCA) and its direction is from ICA to PCA. See Table 1 for other artery abbreviations.

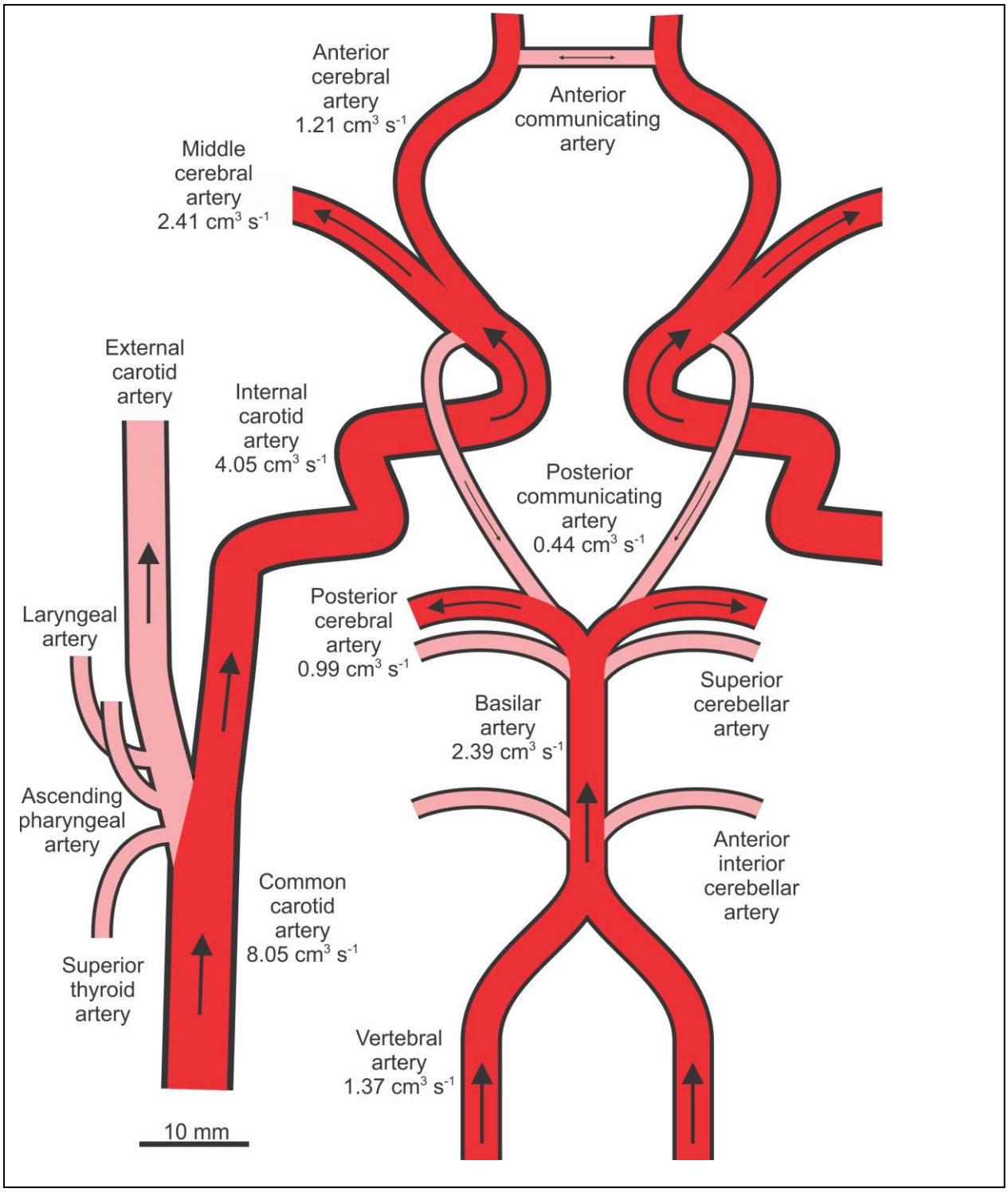


Figure 1. Major arteries of the healthy adult human cephalic circulation joining the Circle of Willis (cerebral arterial circle). Vessel diameters are drawn to scale for the major arteries examined in this study (dark red). Selected smaller arteries (pink; not to scale) are shown but were not directly measured, and other small cephalic arteries are omitted. Mean values of blood flow rate ($\dot{Q}$, $cm^3\ s^{-1}$) are indicated next to each artery on one side only. Data are from Table 1.

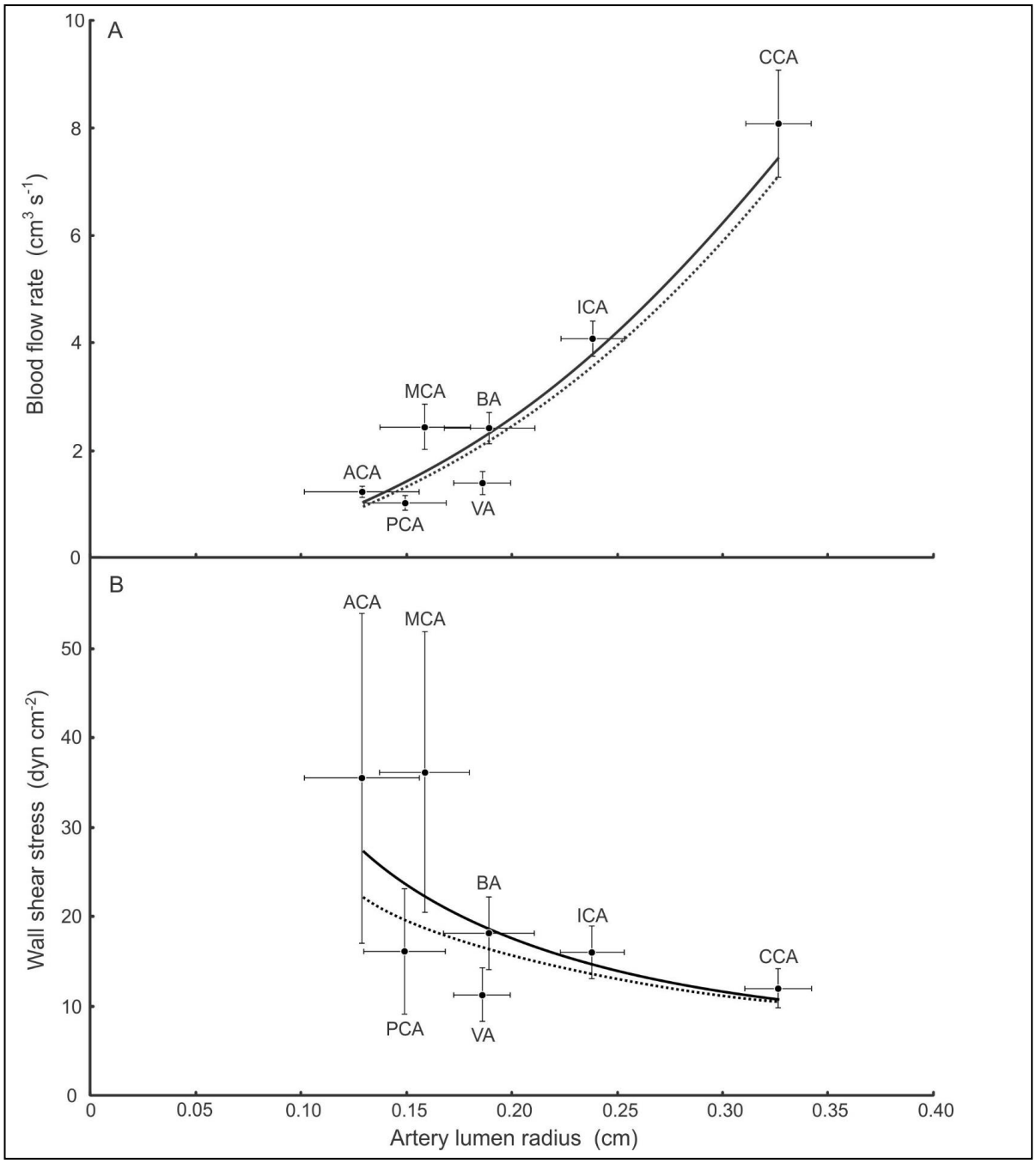


Figure 2. (A) Blood flow rate ($\dot{Q}$, $cm^3\ s^{-1}$) and (B) calculated wall shear stress ($\tau$, dyn $cm^{-2}$) in seven major cephalic arteries in relation to lumen radius ($r_i$, cm) in humans. Means and 95% confidence intervals are presented for the arteries, common carotid (CCA), internal carotid (ICA), basilar (BA), vertebral (VA), middle cerebral (MCA), posterior cerebral (PCA) and anterior cerebral (ACA). The solid lines are least square regressions from means of the present data, where $\dot{Q} = 82.6\ r_i^{2.16}$ and $\tau = 3.44\ r_i^{-1.02}$. The dotted lines represent polynomial regressions from previous analyses for arteries of mammals in general, where $\log \dot{Q} = -0.20 \log r_i^2 + 1.91 \log r_i + 1.82$, and $\log \tau = -0.20 \log r_i^2 - 1.09 \log r_i + 0.53$ (Seymour et al. 2019).

Table 1. Mean ± 95% CI arterial lumen radii, blood flow rates, and calculated wall shear stress (WSS) of single arteries of the human cephalic circulation based on data from 19 PC-MRI and ultrasound imaging studies. Data for exclusively PC-MRI studies are given in Table S1 of the Supplementary Material.

| Artery | Number of studies | Radius ($r_i$, cm) | | Flow rate ($\dot{Q}$, $cm^3\ s^{-1}$) | | WSS ($\tau$, dyn $cm^{-2}$) | |
|---|---|---|---|---|---|---|---|
| SINGLE | N | mean | 95% CI | mean | 95% CI | mean | 95% CI |
| common carotid (CCA) | 7 | 0.327 | 0.016 | 8.05 | 1.00 | 12.0 | 2.2 |
| internal carotid (ICA) | 13 | 0.239 | 0.015 | 4.05 | 0.33 | 16.1 | 3.0 |
| basilar (BA) | 3 | 0.190 | 0.021 | 2.39 | 0.29 | 18.2 | 4.1 |
| vertebral (VA) | 8 | 0.186 | 0.014 | 1.37 | 0.21 | 11.3 | 3.0 |
| middle cerebral (MCA) | 7 | 0.159 | 0.021 | 2.41 | 0.42 | 36.2 | 15.7 |
| posterior cerebral (PCA) | 3 | 0.150 | 0.019 | 0.99 | 0.14 | 16.2 | 7.0 |
| anterior cerebral (ACA) | 5 | 0.129 | 0.027 | 1.21 | 0.10 | 35.5 | 18.5 |

Table 2. Mean total blood flow rates of the paired cephalic arteries of humans (= twice the single flow rates). Also shown are the percentage flow rates relative to total brain blood flow rate.

| Variable | $cm^3\ s^{-1}$ | $cm^3\ min^{-1}$ | % total |
|---|---|---|---|
| Total brain flow rate | 10.8 | 650 | 100 |
| ICA × 2 | 8.1 | 486 | 75 |
| VA × 2 | 2.7 | 164 | 25 |
| (ACA+MCA) × 2 | 7.2 | 434 | 67 |
| (ACA+MCA+PCA) × 2 | 9.2 | 553 | 85 |
| PCoA × 2* | 0.9 | 53 | 8 |

*Posterior communicating artery (PCoA) flow is calculated (ICA – ACA – MCA) and its direction is from ICA to PCA. See Table 1 for other artery abbreviations.